J. Phys. Chem. A **1999,** *103,* 8543−8546

On the Mechanism of the BrO + CH_2O Reaction

Jaron C. Hansen, Yumin Li, and Joseph S. Francisco*

Department of Chemistry and Department of Earth and Atmospheric Science, Purdue University, West Lafayette, Indiana 47907-1393

Zhuangjie Li

Department of Atmospheric Sciences, University of Illinois at Urbana−Champaign, Urbana, Illinois 61801

Received: June 1, 1999; In Final Form: July 30, 1999

The mechanism of the reaction of BrO + CH_2O has been examined using density functional and quadratic configuration interaction molecular orbital methods. The most favorable pathway is found to be the abstraction of hydrogen from CH_2O by BrO radicals. The activation energy barrier for the process is estimated as 2.9 ± 3 kcal mol^{-1}. Results from discharge flow/mass spectroscopy experiments support the finding that the major products of the reaction are HOBr and HCO radicals. The rate of the BrO + CH_2O reaction has been estimated by using transition state theory.

I. Introduction

Bromine compounds from natural and anthropogenic sources play an important role in the chemical processes of the atmosphere. In particular, they are responsible for significant ozone depletion.[1−4] Once these compounds are formed, photolysis and subsequent atmospheric oxidation processes release bromine atoms into the atmosphere. In the Arctic, release of molecular bromine results from heterogeneous reactions on sea-salt aerosols. The subsequent photolysis of molecular bromine produces bromine atoms which react with ozone. The reaction of bromine atoms and ozone is not only efficient in ozone depletion, but it also converts bromine atoms into BrO radicals. During daylight, nearly half of the inorganic bromine in the atmosphere is present in the reactive form of BrO radicals.

$$Br + O_3 \rightarrow BrO + O_2 \qquad (1)$$

Few mechanisms have been proposed for converting the BrO radicals to active bromine atoms. One possible reaction involves the reaction of BrO + CH_2O.

$$BrO + CH_2O \rightarrow HOBr + HCO \qquad (2)$$

Recent studies in the Arctic have shown a correlation between formaldehyde (CH_2O) concentrations and ozone.[5] Current gas-phase models of the chemistry in the Arctic are unable to account for formaldehyde concentrations in ambient measurements.[2,6,7] Given that in the Arctic marine boundary layer most of the reactive bromine is present in the form of BrO, it is possible that a formaldehyde molecule is removed by reaction with BrO radicals.

In addition to removing formaldehyde, the BrO + CH_2O reaction generates HOBr, whose photolysis regenerates bromine atoms.

$$HOBr + h\nu \rightarrow OH + Br \qquad (3)$$

The BrO + CH_2O reaction acts as a sink for the interconversion of reactive forms of bromine. This process could have major implications in understanding ozone destruction cycles in the Arctic by homogeneous gas-phase processes. However, there are currently no experimental measurements for the BrO + CH_2O reaction in the literature. To evaluate whether the BrO + CH_2O reaction acts as an important removal mechanism for formaldehyde and an interconversion mechanism for reactive bromine that forms in the Arctic region, we have used ab initio molecular orbital methods to examine details of the reaction.

II. Computational Methods

Ab initio molecular orbital calculations were performed with the GAUSSIAN 94 series of programs.[8] Geometry optimizations and frequency calculations were carried out using the B3LYP and QCISD methods. The B3LYP method was used along with the 6-31G(d,p) basis set to initially search for the minimum and transition state structures. For all of the species involved in the reaction of BrO with CH_2O, geometries were optimized using Schlegel's method[9] to better than 0.001 Å for bond lengths and 0.01° for bond angles, with a self-consistent field convergence of at least 10^{-9} on the elements of the density matrix. The residual rms force is less than 10^{-4} atomic units. The transition state, which was initially located at the B3LYP/6-31G(d,p) level of theory, was confirmed by a harmonic frequency calculation and shown to exhibit one imaginary harmonic frequency. An intrinsic reaction coordinate (IRC) calculation was performed to check whether the transition state that was located went to the current reactants or products. On the basis of the force constants and optimized geometry obtained at the B3LYP/6-31G(d,p) level of theory, all of the species were reoptimized at the QCISD/6-311G(d,p) level of theory. To improve the energetics, the single-point calculations were also performed for all of the species at the QCISD(T) level of theory with the 6-311G(2d,2p) and 6-311++G(2df,2p) basis sets.

III. Results and Discussion

A. Products of the BrO + CH_2O Reaction. A discharge flow−mass spectroscopy (DF/MS) experiment was performed to determine the products of the BrO + CH_2O reaction. The BrO radicals in this experiment were produced by the reaction of O atoms with Br_2. The O atoms were produced by a microwave discharge of O_2. When BrO radicals were allowed

10.1021/jp991757j CCC: $18.00

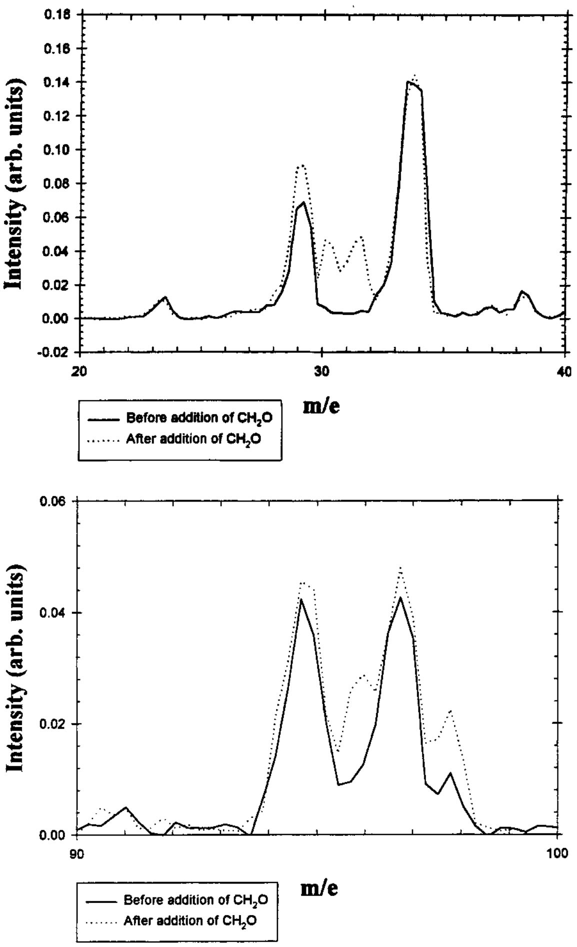

Figure 1. Mass spectrum of the BrO + CH_2O reaction. (a) CHO radical appearance. (b) HOBr appearance.

to react with CH_2O, the products observed from the reaction were HOBr and HCO. This is illustrated in the mass spectrum shown in Figure 1. Both HOBr ($m/e = 96$ and 98) and HCO ($m/e = 29$) were produced on the same time scale. The observed reaction products from the BrO + CH_2O reaction suggest that the major channel involves hydrogen abstraction by the BrO radicals.

B. The BrO + CH_2O Hydrogen Abstraction Reaction. The transition state structure was located along the reaction coordinate of the BrO radical approaching the hydrogen of CH_2O. During the process of searching for the transition state, we found that when the BrO radical approaches the hydrogen of CH_2O at long-range distances, the oxygen of BrO interacts with the hydrogen to form a complex possessing an OH′ distance of 2.571 Å. The geometry of the complex is provided in Table 1. It is seen that the BrO bond length and the CH bond length of CH_2O is not significantly affected as a result of the interaction. The CH′ bond in complex is shortened by 0.003 Å. Vibrational frequency calculations at the QCISD/6-31G(d,p) level (see Table 2) reveal that the complex is at a minimum with all positive frequencies. From the total energies given in Table 3, we find that the complex is weakly bound. At the QCISD(T)/6-311++G(2df,2p)//QCISD/6-31G(d,p) level of theory, with the incorporation of zero point energy calculations, the complex is bound by 1.3 kcal mol^{-1}.

When the BrO is brought further into contact with the hydrogen of the CH_2O, the CH′ bond starts to elongate. At the transition state, the CH′ bond is 1.247 Å. This is only 13% longer than the CH bond in CH_2O. The forming OH′ bond in HOBr in the transition state complex is 1.287 Å, which is 0.319 Å longer than the OH bond distance of 0.968 Å in HOBr. The QCISD/6-31G(d,p) frequency calculation (see Table 2) indicates that the transition state is a first-order saddle point with an imaginary frequency predicted to be at 1971i cm^{-1}. The vibrational analysis of this frequency shows that the motion consists mainly of the OH′ and CH′ stretches. This is consistent with the CH′ bond elongation and OH′ bond formation of the transition state illustrated in Figure 2.

To evaluate the energetics of the BrO + CH_2O reaction, we examined the HO + CH_2O reaction for which there is a wealth of experimental data to compare in order to evaluate the reliability of the ab initio results. The transition state for the HO + CH_2O reaction was found at the QCISD/6-31G(d,p) level of theory, and a frequency calculation verified that it had one imaginary frequency. The geometry of the transition state was used to calculate single-point energies with the QCISD(T) method incorporating the 6-311G(2d,2p) and 6-311++G(2df,2p) basis sets. The total and relative energetics of the HO + CH_2O system are given in Table 4. If we use the experimental heats of formation values at 0 K for HO (9.17 ± 0.29 kcal mol^{-1}), CH_2O (−26.782 ± 1.5 kcal mol^{-1}), H_2O (−57.1 ± 0.0 kcal mol^{-1}), and HCO (10.3 ± 2.5 kcal mol^{-1}), the heat of reaction for the $HO + CH_2O \rightarrow H_2O + HCO$ is found to be −29.2 ± 1.7 kcal mol^{-1}. A comparison of the heat of reaction of −29.7 kcal mol^{-1} calculated at the QCISD(T)/6-311++G(2df,2p)//QCISD/6-31G(d,p) level of theory with that from experiments shows that the calculations overestimate the heat of reaction by 0.5 kcal mol^{-1}. This suggests that the high-level calculations properly predict the heat of reaction for the HO + CH_2O reaction.

To evaluate the validity of the activation energy for the BrO + CH_2O reaction, we examined the HO + CH_2O reaction,[9] which is a similar H-abstraction reaction. The reaction between HO and CH_2O was chosen because of the large number of independent measurements which had been taken to arrive at the Jet Propulsion Lab (JPL) compiled value.[10] There have been several studies of the activation energy barrier for the HO + CH_2O abstraction reaction. Table 4 shows the comparison of theoretical and experimental results for the activation energy of the HO + CH_2O reaction. The JPL compilation[10] evaluation of all the experimental studies suggests that there is no energy barrier for the HO + CH_2O. The reported E/R value is 0 ± 200. We find that there is essentially no barrier within the uncertainty of these calculations. The calculations underestimate the barrier by 0.400 kcal mol^{-1} for the HO + CH_2O reaction, which falls, nevertheless, within the uncertainty range of the experiments. The calibration calculations suggest that the energetics for the BrO + CH_2O reaction should be reasonably predicted at the QCISD(T)/6-311++G(2df,2p)//QCISD/6-31G(d,p) level of theory.

The relative energetics for the BrO + CH_2O reaction is presented in Table 5. The structural changes seen in the transition state suggest that the transition state is early or reactant-like. Such a transition state, as suggested by the Hammond postulate,[11] is indicative of an exothermic reaction. The heat of reaction for the BrO + CH_2O reaction yielding HOBr + HCO is calculated to be exothermic at all levels of theory. These results are consistent with the structural implications from the transition state. At the QCISD(T)/6-311++G(2df,2p)//QCISD/6-31G(d,p) level of theory, the heat of reaction is estimated to be exothermic by −10.3 kcal mol^{-1}. This is about 2.3 kcal mol^{-1} lower than that obtained from experiments. However, there is a 2 kcal mol^{-1} uncertainty in

TABLE 1: Geometries[a] for Species Involved in the BrO+ CH_2O Reaction

species	coordinate	QCISD/6-31G(d,p)	species	coordinate	QCISD/6-31G(d,p)
BrO	BrO	1.781	HOBr	BrO	1.869
				HO	0.968
HCO	CH	1.118		HOBr	102.0
	CO	1.192			
	HCO	124.5	CH_2O	CH	1.101
				CO	1.216
				HCO	122.3
$[BrO + CH_2O]_{cmpx}$	BrO	1.781	$[BrO + CH_2O]^{\ddagger}$	BrO	1.835
	OH′	2.571		OH′	1.287
	CH′	1.098		CH′	1.247
	CO	1.218		CO	1.200
	CH	1.101		CH	1.105
	BrOH′	83.7		BrOH′	102.8
	OH′C	154.1		OH′C	168.7
	H′CO	122.1		H′CO	119.7
	HCO	116.0		HCO	124.2
	BrOH′C	0.0		BrOH′C	0.2
	OH′C′O	0.0		OHCO	−0.2

[a] Bond lengths are given in Å and bond angles are in degrees.

TABLE 2: Harmonic Vibrational Frequencies[a] for Species Involved in the BrO + CH_2O Reaction

species	frequencies (cm^{-1})	ZPE
BrO	677	1.0
HOBr	3845, 1213, 616	8.1
HCO	2770, 1890, 1167	8.3
CH_2O	3075, 3006, 1826, 1587, 1299, 1214	17.2
$[BrO + CH_2O]_{cmpx}$	3107, 3017, 1816, 1590, 1308, 1233, 681, 184, 155, 81, 56, 50	19.0
$[BrO + CH_2O]^{\ddagger}$	2993, 1882, 1564, 1238, 1119, 701, 586, 331, 296, 94, 89, 1971i	15.5

[a] Harmonic frequencies are calculated at the QCISD/6-31G(d,p) level of theory.

TABLE 3: Total Energies (hartrees) for Species Involved in the BrO + CH_2O Reaction

	QCISD	QCISD(T)[a]	
species	6-31G(d,p)	6-311G(2d,2p)	6-311++G(2df,2p)
BrO	−2644.93241	−2647.49337	−2647.55691
HOBr	−2645.58676	−2648.15486	−2648.21894
HCO	−113.55348	−113.64194	−113.67904
CH_2O	−114.19890	−114.28827	−114.32752
$[BrO + CH_2O]_{cmpx}$	−2759.13682	−2761.78554	−2761.88776
$[BrO + CH_2O]^{\ddagger}$	−2759.11644	−2761.77322	−2761.87537

[a] Single-point energies calculated with the QCISD/6-31G(d,p) geometry.

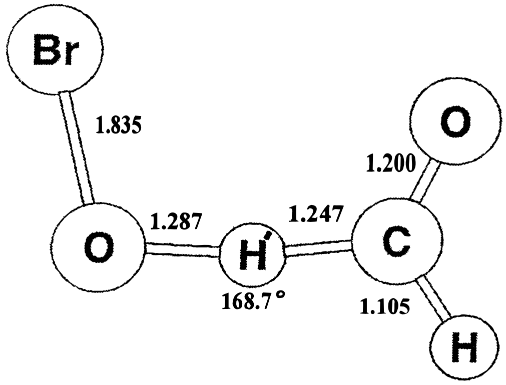

Figure 2. Transition state structure for the reaction of BrO + CH_2O → HOBr + HCO.

TABLE 4: Total (hartrees) and Relative Energetics (kcal mol^{-1}) for Species Involved in the HO + CH_2O Reaction

Total Energies for Species in the HO + CH_2O Reaction

	QCISD	QCISD(T)	
species	6-31G(d,p)	6-311G(2d,2p)	6-311++G(2df,2p)
HO	−75.54689	−75.60822	−75.63361
H_2O	−76.22895	−76.29907	−76.32847
$[HO + CH_2O]^{\ddagger}$	−189.73946	−189.89622	−189.96218

Relative Energetics for the HO + CH_2O Reaction

level of theory	HO + CH_2O → H_2O + HCO	HO + CH_2O → $[HO + CH_2O]^{\ddagger}$
QCISD/6-31G(d,p)	−22.9	4.0
QCISD(T)/6-311G(2d,2p)	−27.9	0.2
QCISD(T)/6-311++G(2df,2p)	−29.1	−0.6
ΔZPE	−0.6	0.2
QCISD(T)/6-311++G(2df,2p)+ΔZPE	−29.7	−0.4 ± 3
exptl	−29.2 ± 1.7	0 ± 0.4

the BrO heat of formation value used from JANAF.[12] Using E_o(G2) values from the literature[14,15] for all four reactants and products for the BrO + CH_2O reaction, the G2 heat of reaction is calculated to be −10.6 kcal mol^{-1}. We find that the heats of reaction calculated at the QCISD(T)/6-311++G(2df,2p)//QCISD/6-31G(d,p) level of theory, and with the G2 method, are in excellent agreement. The calculated barrier height for the hydrogen abstraction reaction of BrO + CH_2O is estimated to be 2.9 kcal mol^{-1}. After correcting for tunneling (−1.1 kcal mol^{-1}, Wigner correction[16] based on 1971i cm^{-1}), a best estimate of the activation barrier of 1.8 kcal mol^{-1} is obtained. The relative energetics for the BrO + CH_2O reaction at the QCISD(T)/6-311++G(2df,2p)//QCISD/6-31G(d,p) level of theory is illustrated in Figure 3.

C. Estimation of the Rate Constant for the BrO + CH_2O Reaction. With the calculated barriers, vibrational frequencies, and rotational constants for the HO + CH_2O and BrO + CH_2O reactions, we estimated the rate constants for both reactions using transition state theory (TST). The basic postulate of transition state theory is that the rate of transformation of the reactants to products is given solely by the passage, in the forward direction, of reactants through the transition state and then onto products. Calculation of the partition functions for the transition state and reactants coupled with the activation energy then yields a thermal rate constant. This is given by the following equation:

$$k(T) = (k_B T/h)*(Q^{\ddagger})/(Q_A Q_B)*\exp(-E_o/k_B T) \qquad (4)$$

TABLE 5: Relative Energetics for the BrO + CH_2O Reaction

	relative energetics (kcal mol^{-1})		
level of theory	BrO + CH_2O → HOBr + HCO	BrO + CH_2O → $[BrO + CH_2O]_{cmpx}$	BrO + CH_2O → $[BrO + CH_2O]^{\ddagger}$
QCISD/6-31G(d,p)	−5.6	−3.5	9.3
QCISD(T)/6-311G(2d,2p)	−9.5	−2.4	5.3
QCISD(T)/6-311++G(2df,2p)	−8.5	−2.1	5.6
ΔZPE	−1.8	0.8	−2.7
QCISD(T)/6-311++G(2df,2p) + ΔZPE	−10.3	−1.3	2.9
exptl	−4.05 ± 1.9		

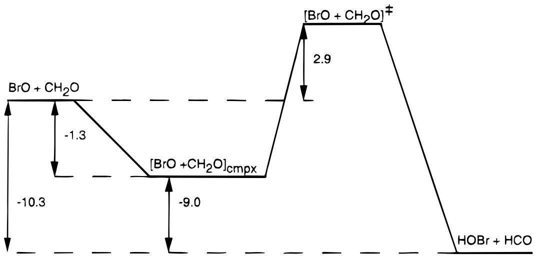

Figure 3. Relative energetics for the BrO + CH_2O reaction at the QCISD(T)/6-311++G(2df,2p)//QCISD/6-31G(d,p) level of theory.

TABLE 6: Comparison of Experimentally Determined A-Factor for OH + CH_2O

experimentally determined A-factor[a]	reference
1.25×10^{-11}	*b*
6.00×10^{-11}	*c*
1.66×10^{-11}	*d*
1.00×10^{-11}	*e*
1.25×10^{-11}	*f*

[a] A-factors are in units of cm^3 $molecule^{-1}$ sec^{-1}. [b] Atkinson, R.; Pitts, J. N. *J. Chem. Phys.* **1978**, *68*, 3581. [c] Smith, R. H. *Int. J. Chem. Kinet.* **1978**, *10*, 519. [d] Zabarnick, S.; Fleming, J. W.; Lin, M. C. *Int. J. Chem. Kinet.* **1987**, *20*, 117. [e] DeMore, W. B.; Sander, S. P.; Golden, D. M.; Hampson, R. F.; Kurylo, M. J.; Howard, C. J.; Ravishankara, A. R.; Kolb, C. E.; Molina, M. J. JPL Publication 94-26. [f] Stief, L. J.; Nava, D. F.; Payne, W. A.; Michael, J. V. *J. Chem. Phys.* **1980**, *73*, 5.

$Q^{\ddagger}$ is the partition function for the transition state, Q_A and Q_B are the partition functions for the reactants A and B, k_B is the Boltzmann constant and h is Plank's constant. To evaluate the validity of the rate constant calculated solely from ab initio parameters, a calibration calculation was first carried out on the HO + CH_2O reaction. From the geometries and vibrational frequencies for the reactants (HO + CH_2O) and the abstraction transition state, the partition coefficients are calculated. Using the above equation, the A-factor can be calculated. Table 6 is a comparison of the experimentally determined preexponential A-factor and rate constant for HO + CH_2O. The recommended preexponential A-factor from the JPL compilation is 1.00×10^{-11} cm^3 $molecule^{-1}$ s^{-1}. From the ab initio parameters including corrections for tunneling, we estimate a preexponential A-factor of 6.21×10^{-12} cm^3 $molecule^{-1}$ s^{-1}. There is a difference of 38% between the experimental value and the calculated value, which can be attributed to the uncertainty in the calculated rotational constants and vibrational frequencies found in the calculations. This exercise also shows that a reasonable preexponential A-factor value could be determined solely from ab initio calculations.

From our examination of the preexponential A-factor from the HO + CH_2O reaction, we find that it may be necessary to scale the calculated results from the ab initio calculations to match the experimental observation. This suggests that, to obtain a reasonable estimate of the preexponential A-factor for the BrO + CH_2O reaction, it may be necessary to scale the preexponential A-factor. In this case, if we use the scale factor derived from the HO + CH_2O reaction, the estimated preexponential A-factor for the BrO + CH_2O reaction is 6.3×10^{-13} cm^3 $molecule^{-1}$ s^{-1} at 298 K. This result for the BrO + CH_2O reaction is not unreasonable. The estimated kinetic rate constant for the BrO + CH_2O reaction is 1.5×10^{-14} cm^3 $molecule^{-1}$ s^{-1} at 298 K. This value represents an average of rates over the range of activation energy barrier for the BrO + CH_2O reaction. The results suggest that the BrO + CH_2O reaction is slow.

IV. Summary

Ab initio molecular orbital calculations were performed in order to study the BrO + CH_2O reaction. The calculations suggest that the reaction proceeds by hydrogen extraction from CH_2O. Experimental results performed using discharge flow/mass spectroscopy verify the calculated results, showing the products of the reaction to be HOBr and HCO. At the highest level of theory [QCISD(T)/6-311++G(2df,2p)], the activation energy was calculated to be 2.9 kcal mol^{-1}, without tunneling corrections. When corrected for tunneling, the activation energy barrier was estimated to be 1.8 kcal mol^{-1}. The rate constant for the BrO + CH_2O reaction was estimated using transition state theory and was calculated to be 1.5×10^{-14} cm^3 $molecules^{-1}$ s^{-1}.

References and Notes

(1) Barrie, L. A.; Bottenheim, J. W.; Schnell, R. C.; Crutzen, P. J.; Rasmussen, R. A. *Nature* **1988**, *334*, 138.

(2) McCounell, J. C.; Henderson, G. S.; Barrie, L. A.; Buttenheim, J. W.; Niki, H.; Langford, C. H.; Templeton, E. M. J. *Nature* **1992**, *355*, 150.

(3) Le Bras, G.; Platt, U. *Geophys. Res. Lett.* **1995**, *22*, 599.

(4) Wessel, S. *Berichte zur Polarforschung* 224, 1977.

(5) Shepson, P. B.; Sumner, A. L. *Nature* **1999**, *398*, 230.

(6) Shepson, P. B.; Sirju, A. P.; Hopper, J. F.; Barrie, L. A.; Young, V.; Niki, H.; Pryflout, H. *J. Geophys. Res.* **1996**, *101*, 21081.

(7) Sander, R.; Vogt, R.; Harris, G. W.; Grutzen, P. J. *Tellus* **1997**, *49B*, 522.

(8) Frish, M. J.; Trucks, G. W.; Schlegel, H. B.; Gill, P. M. W.; Johnson, B. G.; Robb, M. A.; Cheeseman, J. R.; Keith, T.; Peterson, G. A.; Montgomery, J. A.; Raghavachari, K.;. Al-Laham, M. A.; Zakrewski, V. G.; Ortiz, J. V.; Foresman, J. B.; Cioslowski, J.; Stefanov, B. B.; Nanayakkara, M. Challacombe; Peng, C. Y.; Ayala, P. Y.; Chen, W.; Wong, M. W.; Andres, J. L.; Replogle, E. S.; Gomperts, R.; Martin, R. L.; Fox, D. J.; Binkley, J. S.; Defrees, D. J.; Baker, J.; Stewart, J. P.; Head-Gordon, M.; Gonzalez, C.; Pople, J. A. *Gaussian 94*, Revision D.2; Gaussisn, Inc.: Pittsburgh, PA, 1995.

(9) Schlegel, H. B. *J. Comput. Chem.* **1982**, *3*, 214.

(10) Poulet, G.; Le Bras, G.; Lombourien, J. *Geophys. Res. Lett.* **1980**, *7*, 413.

(11) DeMore, W. B.; Sander, S. P.; Golden, D. M.; Hampson, R. F.; Kurylo, M. J.; Howard, C. J.; Ravishankaran, A. R.; Kolb, C. E.; Molina, M. J., JPL Publication 94-26.

(12) Hammond, G. S. *J. Am. Chem. Soc.* **1955**, *77*, 334.

(13) Chase, M. W.; Davies, C. A.; Downey, J. R.; Frurie, D. J.; McDonald, R. A.; Syrerud, A. N. *J. Phys. Chem. Ref. Data Suppl. 1* 1985.

(14) Blaudeau, J. P.; McGrath, M. P.; Curtiss, L. A.; Radom, L. *J. Chem. Phys.* **1997**, *107*, 5016.

(15) Curtiss, L. A.; Raghavachari, K.; Trucks, G. W.; Pople, J. A. *J. Chem. Phys.* **1991**, *94*, 7221.

(16) Wigner, E. P. *Z. Phys. Chem. Abst.* **1932**, *B19*, 293.